

Received 22 October 2023, accepted 23 December 2023, date of publication 9 January 2024,  
date of current version 26 January 2024.

Digital Object Identifier 10.1109/ACCESS.2024.3351708

## RESEARCH ARTICLE

# Robust PID Control of EV Aggregator for C-FCAS Using Sequential Multi-Objective Optimization

ADLAN BAGUS PRADANA<sup>1</sup>, (Student Member, IEEE),

MD. MEJBAUL HAQUE<sup>1</sup>, (Senior Member, IEEE),

AWAN UJI KRISMANTO<sup>2</sup>, (Member, IEEE),

HERLAMANG SETIADI<sup>3</sup>, (Member, IEEE),

AND MITHULAN NADARAJAH<sup>1</sup>, (Senior Member, IEEE)

<sup>1</sup>School of Electrical Engineering and Computer Science, The University of Queensland (UQ), St Lucia, Brisbane, QLD 4072, Australia

<sup>2</sup>Department of Electrical Engineering, Institut Teknologi Nasional Malang, Malang 65152, Indonesia

<sup>3</sup>Faculty of Advanced Technology and Multidiscipline, Universitas Airlangga, Surabaya 60115, Indonesia

Corresponding author: Adlan Bagus Pradana (a.pradana@uq.edu.au)

This work was supported in part by the Indonesia Endowment Funds for Education (LPDP).

**ABSTRACT** Integrating Electric Vehicles (EVs) charging into power grids through EV aggregator, offers promising benefits to society for reliable, sustainable, and cost-effective energy solutions. A key aspect of this integration is the possibility of provision of Contingency-Frequency Control Ancillary Services (C-FCAS). While EVs primarily serve owners' transportation needs, they must return to their idle positions with a satisfactory State of Charge (SoC) after providing frequency support following a contingency. However, real-world implementations of grid-connected EV aggregator control for C-FCAS are complex and challenging because several factors, including uncertainties, perturbation magnitude, renewable energy penetration, and the SoC of EVs need to be considered. To implement the C-FCAS considering these factors, this paper presents a robust PID control approach for an EV aggregator. The objective is to effectively manage EV units willing to participate, ensuring frequency regulation support, system stability, and smooth return to their idle position. The strategy exploits a sequential multi-objective optimization approach with two main objectives: mitigating frequency perturbations caused by contingencies and restoring EV units power discharge to zero after a critical time period. Sequential Multi-objective Optimization (SMO) algorithms optimize the control parameters under diverse scenarios and uncertainties. The simulation results validate the effectiveness of the proposed strategy. The control strategy by an EV aggregator successfully handled different market conditions and uncertainties, ensuring reliable frequency regulation. This service opportunity will enhance income of EV owners and their willingness to participate while helping to keep the integrity of system operation.

**INDEX TERMS** Electric vehicles (EV), EV aggregator, contingency-frequency control ancillary service (C-FCAS), sequential multi-objective optimization (SMO), robust PID control.

## I. INTRODUCTION

The grid incorporation of electric vehicles (EVs) in electric power grids has attracted significant attention in recent years because of their ability to offer sustainable and efficient energy solutions [1], [2]. In the context of the electrical system, a single electric vehicle (EV) might appear incon-

The associate editor coordinating the review of this manuscript and approving it for publication was Mou Chen<sup>1</sup>.

sequential, but when multiple EVs are plugged in at specific locations like commercial centers or universities, they transform into substantial energy resources for the grid. An EV aggregator plays a crucial role as an intermediary between these EVs and the system operator [3].

EV aggregator could offer the opportunity to contribute to the grid by providing ancillary services such as frequency control [4]. This service is formalized under the term "Frequency Control Ancillary Services" (FCAS), which can be

further classified into two subcategories: regulation, denoted as R-FCAS, and contingency, denoted as C-FCAS. While R-FCAS services are continually employed to make minor, C-FCAS services are specifically designed to address unforeseen contingency events only. C-FCAS involves utilizing the flexibility of EV aggregator to support grid frequency during contingencies while ensuring that the primary function to meet energy requirements of EV.

Nevertheless, the successful integration of EV aggregator into the power grid for C-FCAS applications presents various challenges. Uncertainties such as the scale of perturbations, renewable energy infiltration, and State of Charge (SoC) of EVs introduce complexities that must be addressed for effective control and operation [5]. To overcome these challenges, this study presents a robust PID control strategy for EV aggregator employed in C-FCAS using Sequential Multi-objective Optimization (SMO).

SMO is an approach that sequentially addresses the optimization of multiple conflicting objectives. Often, multiple objectives need to be simultaneously optimized, but these objectives may struggle with each other. For example, minimizing the frequency deviations and restoring them to their idle state in an EV aggregator as a C-FCAS scenario. SMO aims to find a set of resolutions that represent the trade-off between these conflicting objectives. Instead of trying to find a single optimal solution that pleases all objectives simultaneously, SMO iteratively improves the solutions by focusing on one objective at a time. The idea is to optimize one objective while keeping the others fixed, and then switch to optimizing the next objective while considering the previously optimized objectives.

The fast response of EV aggregator to frequency contingencies has the potential to provide sufficient transition time between EV aggregator and the main generator. This, in turn, can simplify the generator control and reduce maintenance requirements [6], [7]. Furthermore, given the similarities in operation, it is possible to extend the proposed control strategy to other FCAS technologies, such as Battery Energy Storage Systems (BESS) and Flywheel Energy Storage Systems (FESS) [8].

The remainder of this paper is organized as follows. Section II presents a comprehensive review of the relevant literature, highlighting the challenges and existing methodologies for integrating EV aggregator and C-FCAS. Section III provides an overview of the modelling approach used in this study, laying the foundation for subsequent control strategy implementations. Section IV presents a detailed presentation of several control strategies that are applied and analyzed in this research. Section V elaborates the methodology employed to optimize the control parameters. In Section VI, the simulation setup is detailed and the results obtained from the simulations are thoroughly analyzed and discussed. The implications of the proposed strategy and its potential applications were examined, providing valuable insights into its real-world effectiveness. Finally, Section VII concludes the paper by summarizing the contributions of

this study and offering suggestions for future research directions.

## II. LITERATURE REVIEW

Article [9] proposed a coordinated control of EVs and renewable energy sources for frequency regulation, which can adaptively change the control parameters according to system operations and achieve special stabilizing effects compared to a conventional fixed PI controller. The proposed adaptive coordinated controller has potential applications in grids with wind farms (WF), photovoltaics (PV), and EVs, and can be an alternative control resolution for supportive renewable energy sources. Reference [10] suggested a control strategy based on a VSG control technique for an EV used as a transportable energy-storage device to contribute to the frequency regulation of a grid in an independent operation mode. Simulation examples verify the proposed control method and demonstrate excellent dynamic performance. However, its application range is limited to the frequency regulation of a grid in a self-governing operation approach. A report [11] presented an optimal control technique for the EV contribution to frequency regulation in variable power system operating states. The simulation showed that the proposed model resulted in a cost reduction for frequency regulation in a standard state of operation and significantly improved the regaining time for frequency and frequency deviation in an abnormal state of operation. The research presented in [12] developed an optimal management strategy to schedule EVs' charging/discharging procedure of EVs to improve the frequency stability of grids under autonomous operating conditions. Using this strategy, EVs can act as energy storage arrangements to absorb or inject surplus/shortage of energy and improve the frequency variation of grids in the isolated mode, leading to increased profit and decreased emissions for the grid operator. Analysis [13] exhibited an MILP-based tiered control strategy for Secondary Frequency Regulation (SFR) using EVs, aiming to minimize grid frequency deviations, reduce battery degradation, and increase incentives for EV participation in the regulation market. The proposed scheme was experimentally validated and found to have superior performance compared to the existing scheme.

The investigation reported in [14] introduced an EV charging/discharging strategy that minimizes DC microgrid network losses and EV battery degradation through a two-stage optimization framework. The simulations showed significant reductions in system losses and Distributed Generator (DG) capacity, and further investigation is planned for large-scale networks and significant EV uptake. The proposed coordinated controller based on the Multivariable Generalized Predictive Controller (MGPC) concept for Load Frequency Control (LFC) in an isolated microgrid using the V2G technique has shown better robust performance [15]. The proposed method can be used in diverse microgrid configurations, and the feasibility of implementing the proposed method in actual power systems was demonstrated. However,

future work needs to study bus voltage regulation by governing the reactive power with smart solutions. In addition, communication delays may affect the performance of the controller, which poses further challenges and research directions. A bi-level coordination scheme of several aggregators to level the load shape of a distribution system applying the V2G system was proposed in [16]. The scheme was verified on an actual MV distribution system in Korea, using actual traffic density information. The results showed improved peak-shaving and valley-filling performance while fulfilling EV SoC requirements and adapting to the penetration of renewables. Three-layered harmonized control for integrating three-phase AC and DC EV energy storage systems into a hybrid AC/DC grid is recommended [17]. A multilayered management algorithm was implanted into the grid central regulator. Extensive case studies with real-life information show that the proposed controller is effective, reliable, and robust for various scenarios, including homogeneous and heterogeneous single-phase EV charging and synchronization throughout the transition from the islanded to grid-tied mode. A bidirectional charging strategy for EVs in an industrial grid to regulate frequency using grid and charger controllers has been proposed [18]. The results demonstrate that the bidirectional charging strategy significantly improves the frequency regulation and supports active and reactive power, making it a suitable solution for industrial grids with EV integration.

The proposed controller with V2G technology in [19] integrates EVs into the grid to eradicate frequency oscillations and quickly control the system frequency. Simulation results show that the proposed primary frequency controller using Fractional Order PID (FOPID) and V2G technology effectively regulates frequency within an acceptable margin. Furthermore, increasing the number of EV in the grid further improves frequency regulation. An innovative frequency support approach to regulate the operation of distributed energy sources (DES) and manageable loads, such as EVs, to address grid frequency fluctuations has been proposed [20]. The proposed modified droop controller (MDC) dispatches reference signals to both the DES and EVs, and is improved with communication links and feedback mechanisms. Extensive simulations were performed using the planned arrangement of the MG data from Santa Rita Jail.

A graded energy management structure for islanded grids that models grid frequency control functions using droop control and virtual inertia ideas has been proposed [21]. The system also incorporates demand response programs for grid loads and uses scenario-based stochastic programming to handle the uncertainties. The results confirm that the proposed system can successfully enhance grid security, reduce operational costs and emissions, and manage DG resources with higher degrees of freedom. An innovative strategy for charging and discharging EVs in the presence of renewable resources has been endorsed [22]. A cost signal is obtained based on the day-ahead load and the generation of renewables

to manage the EVs' charging and discharging processes. For the EVs to respond to frequency deviations in the charging and discharging processes, four modes were defined. The results showed that the projected approach successfully decreased the frequency deviations and improved the power reserve of the grid. A multi-agent control arrangement for primary frequency control in AC grids with EVs' participation was justified [23]. Simulation studies show that the proposed droop-based method effectively maintains the frequency nadir above the minimum allowed value and returns the steady-state frequency back to a satisfactory level while reducing the stress on other generating units.

An operational planning framework for a grid comprising logistics distribution systems and renewable energy resources has been considered [24]. The model improves the drive paths of EVs, charging/discharging power, and time durations of charging to minimize deviations in the bidding power and actual power output of the grid, considering the stochastic features of wind power and load variations. Simulation results demonstrate that the proposed model can significantly decrease the operational cost of the network by smoothing wind power fluctuations through the coordinated dispatch of EVs while also providing insights on how to control EV charge/discharge and select travel directions. An evaluation [25] determined a control strategy using EVs to provide quick active power support to a grid, which can mitigate the frequency deviation caused by the fluctuating load. The method senses frequency variations and communicates with an EV aggregator to stream the required quantity of active power to the grid, encouraging results in critical parameters, such as settling time and peak over/undershoot.

An ordered optimal dispatch strategy for EVs and Thermostatically Controlled Loads (TCLs) is tested [26]. The simulation results of the IEEE-30 bus system demonstrate that the grouping of EVs and TCLs with the projected dispatch approach achieves the best performance, improving the centralized dispatch of thermal and wind generation and reducing carbon emissions by maximizing wind generation. The proposed model [27] considers EVs and evaluates various scenarios, demonstrating that while vehicle-to-grid (V2G) implementation had minimal benefits, the controlled charging of EVs proved to be highly important in cost reduction. The current implementation is robust and ready for integration into practical systems, offering fast and effective control for both small and large grid operators. A comprehensive demand response (DR) strategy for frequency regulation in grids, considering the presence or absence of wind power generation, has been introduced [28]. The proposed strategy effectively reduces frequency deviations using an Adaptive Hill Climbing (AHC) controller after sudden disturbances, reduces the manipulation of responsive loads to maintain the frequency within the desired range during steady state, and demonstrates stability with a latency of up to 300 ms between the utility control center and the responsive loads. Therefore, there is a need to improve the quality of service for customers.

Existing research has made notable progress in optimizing the mitigation of frequency deviations; however, it has largely overlooked the critical aspect of EVs returning to idle conditions after providing ancillary services [25]. Although a single objective function is sufficient for managing system frequency deviations, it is essential to recognize that EVs are primarily designed for transportation purposes, and their temporary involvement in ancillary services necessitates careful consideration. Moreover, previous studies have not adequately addressed the uncertainties that may arise in real-world scenarios. Factors such as varying magnitudes of disturbances, renewable energy penetration, and EV SoCs have not been thoroughly accounted for. These uncertainties pose significant challenges that must be addressed to ensure robust and effective integration of EV aggregator into ancillary services.

To address the gaps and challenges in integrating EV aggregator into the power grid, this paper proposes a comprehensive approach that prioritizes the return of EV aggregator to idle conditions after providing ancillary services. Unlike previous methods that rely on a single objective function, the proposed approach adopts multi-objective optimization techniques to simultaneously address system frequency deviations and EV aggregator power discharge. Second, by recognizing the uncertainties prevalent in real-world scenarios, this study introduced a robust PID control solution. This means that the results obtained through multi-objective optimization can effectively handle various potential scenarios, encompassing fluctuations in disturbance magnitudes, renewable energy penetration levels, and EV SoC. By embracing uncertainties and prioritizing robustness in the control strategy, the proposed approach enhances the reliability and adaptability of EV aggregator for providing ancillary services. Third, in pursuit of optimal outcomes, several optimization algorithms were tested, including Sequential Quadratic Programming (SQP), Simplex, Interior Point (IP), and Pattern Search (PS), in conjunction with the SMO technique. Finally, to gain deeper insight into EV battery behavior, a quadratic regression model of the Partnership for a New Generation of Vehicles (PNGV) was employed [29]. The utilization of this advanced model enhances the understanding of EV battery dynamics and aids in refining control strategies.

### III. MODELLING AND BACKGROUND

#### A. MODERN POWER SYSTEM

Modern power grids experience high infiltration of Variable Renewable Energy Sources (VRES) PV panels and wind turbines [30], [31]. The high penetration of renewable energy sources presents several benefits and challenges [32]. One key advantage is the potential for carbon emissions reduction and environmental sustainability. Additionally, renewable energy sources generate clean electricity, contributing to a greener and more sustainable energy mix. Moreover, the decentralized nature of VRES allows for improved grid resilience, reliability, and potential energy

independence. However, highly penetrating VRES poses unique challenges. The intermittent and unpredictable nature of renewable energy sources such as solar and wind power can lead to significant fluctuations in power generation [33]. This variability can impact stability, particularly in frequency regulation. Maintaining the grid frequency within acceptable limits ensures reliable and resilient power supply.

With the advancements in energy storage system (ESS) technology, including battery Energy Storage Systems (BESS), ultra-capacitor energy storage (UCES), and the potential utilization of EVs as Energy Storage (EVES), these systems have the opportunity to play a significant role in grid operations [34], [35]. Although individual EVs may have limited storage capacity when managed by an aggregator, a fleet of EVs can collectively serve as a substantial energy storage resource for the grid [36], [37]. A typical modern power grid is depicted in Figure 1, and its high-level control block diagram is shown in Figure 2.

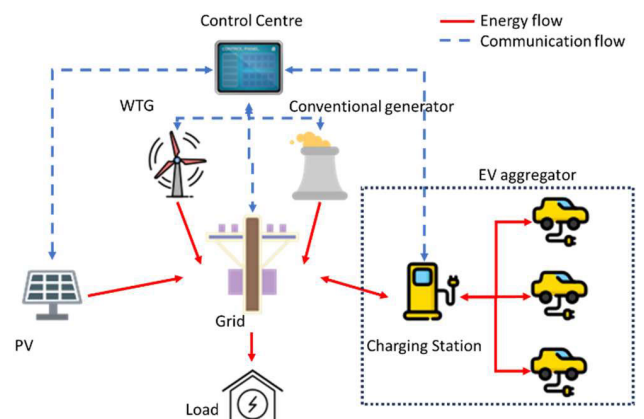


FIGURE 1. Typical of the modern power grid.

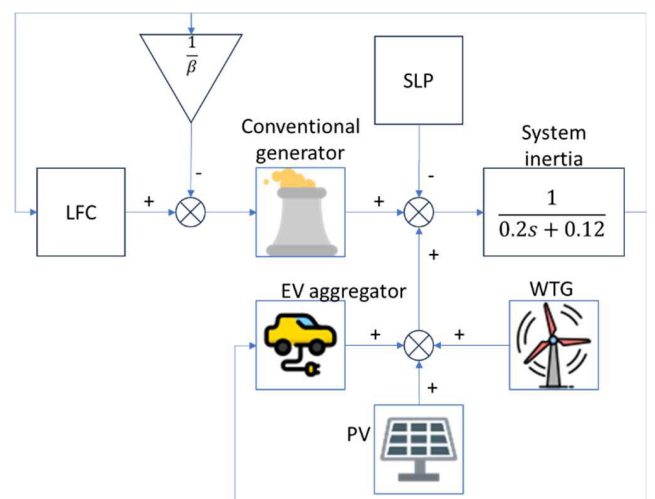


FIGURE 2. Dynamic model of the modern power grid.

**B. ANCILLARY SERVICES MARKET**

Ancillary services encompass electricity-related products that go beyond those typically traded in traditional wholesale electricity markets [38]. These services are additional components of the electricity system that support its reliable operation and include various functions, such as frequency regulation, voltage control, and system reserves. Ancillary services play a crucial role in maintaining grid stability, managing imbalances between electricity supply and demand, and ensuring the overall reliability of power systems.

In the Australian market, the Australian Energy Market Operator (AEMO) classifies ancillary services into three main categories: Network Support and Control Ancillary Services (NSCAS), Frequency Control Ancillary Services (FCAS), and system restoration Ancillary Services (SRAS) [39]. NSCAS encompasses various services for maintaining the stability and control of the network. This includes voltage control, power flow control, and measures to improve the transient and oscillatory stability. As mentioned earlier, the FCAS is further divided into two subcategories: regulation (R-FCAS) and contingency (C-FCAS). R-FCAS services are continuously utilized to make minor adjustments and ensure system stability in response to changes in the supply and demand. By contrast, C-FCAS services are designed to address contingency events and provide support during unexpected system disruptions. Six distinct markets within the C-FCAS category, each with different response times. These markets are fast raise (6-sec raise), fast lower (6-sec lower), slow raise (60-sec raise), slow lower (60-sec lower), delayed raise (5-min raise), and delayed lower (5-min lower), as depicted in Figure 3. Given the dynamic nature of power system requirements, there is a potential for the development of the current ancillary services market.

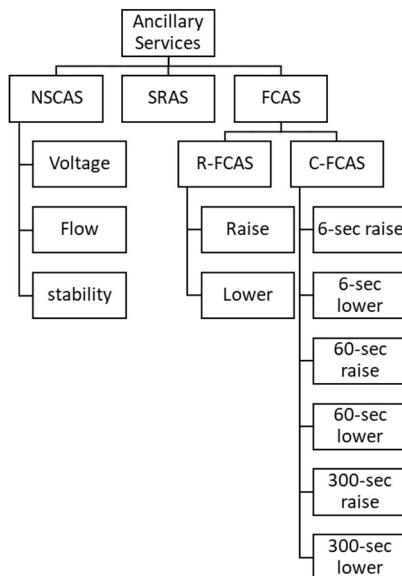


FIGURE 3. AEMO ancillary service classification [39].

**C. EV AGGREGATOR CONTROL FRAMEWORK**

An aggregator plays a crucial role as an intermediary between EV and the grid, simplifying the management process for network operators who would otherwise have to handle a multitude of individual EVs. When an EV is charging, the aggregator sells energy from the grid to the EV, and during discharging, this process is reversed. To fulfill its intermediary function effectively, the aggregator must establish a robust control framework. This framework encompasses tasks such as capacity forecasting, price bidding, and contingency scenario planning. By efficiently managing these aspects, the aggregator ensures the seamless flow of energy between the grid and EVs, optimizing the overall functioning of the electric vehicle ecosystem. The flowchart of this control framework is depicted by Figure 4.

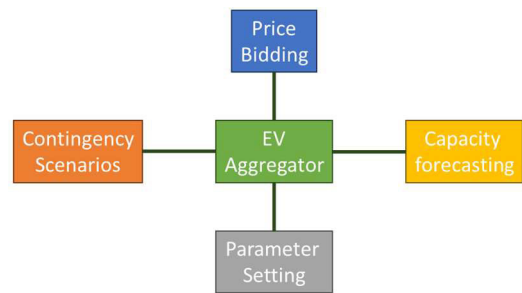


FIGURE 4. Aggregator control framework.

The accurate prediction of the number of EV connected to the aggregator is paramount, as it dictates the energy capacity that the aggregator commits to the network operator. This forecasted data also plays a pivotal role in determining the price of services to be bid to the network operator, ensuring a fair and competitive market environment. Moreover, the aggregator must anticipate various contingency scenarios. Through meticulous simulations that factor in both the number of connected EVs and the aggregator’s capacity, optimal control parameters are established. These parameters are essential, as they govern the aggregator’s responses during unforeseen events, guaranteeing a resilient and adaptive energy distribution system. By considering these elements, the aggregator can make informed decisions, ensuring efficient energy management and enhancing the reliability of the electric vehicle network. Process before aggregator deliver C-FCAS is illustrated by Figure 5.

**D. CONVENTIONAL FOSSIL-BASED GENERATOR**

Conventional fossil-based plants or generators are power generation facilities that rely on the combustion of fossil fuels, such as coal, natural gas, or oil, to harvest electricity [40]. These plants typically consist of turbines, generators, and auxiliary systems designed to convert thermal energy released by burning fossil fuels into electrical energy.

Generators play a specific role in penetrating highly renewable power grids. They are utilized as backbone sources of electricity to ensure a reliable power supply and grid

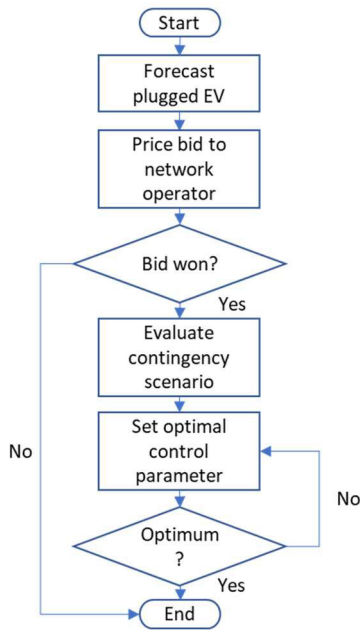


FIGURE 5. Aggregator C-FCAS initial process flowchart.

stability. The two first-order subsystems represent a generator, as shown in Figure 6.

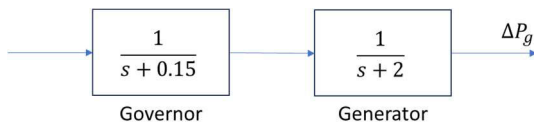


FIGURE 6. Dynamic model of the generator.

Generators provide a consistent and controllable power output, allowing them to compensate for the intermittent nature of renewable energy sources, such as wind or solar energy. When there is a shortfall in renewable energy generation owing to weather conditions or variability, a generator can quickly ramp up its power output to meet the electricity demand and maintain grid stability.

### E. WIND TURBINE GENERATOR

A wind turbine generator (WTG) is a device that translates the kinetic energy from the wind into electrical energy. It typically consists of a rotor with multiple blades that capture wind energy and rotate a generator to produce electricity [41]. WTGs are designed to harness wind power and convert it into electricity without relying on fossil fuel. The wind energy captured by the rotor blades is transformed into mechanical energy, which is then converted into electrical energy. This renewable energy source offers several advantages, including reduced carbon emissions, renewable resource utilization, and energy independence. Owing to the inherent uncertainty in wind energy, WTGs can be modelled by incorporating a white noise signal filtered through a low-pass filter. This

modelling technique allows the consideration of stochastic variations in wind speed and direction, which affect the power output of the WTGs. By incorporating this uncertainty factor, a more realistic representation of WTG performance can be obtained, enabling improved analysis and optimization of wind power systems, as shown in Figure 7 [42].

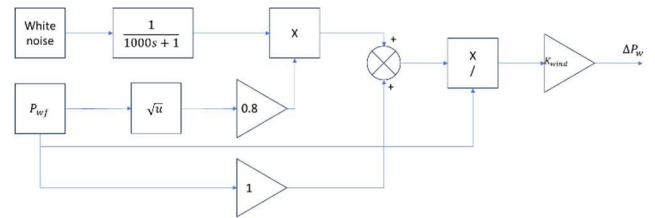


FIGURE 7. Dynamic model of the wind turbine generator.

WTGs provide a significant portion of the electricity supply in highly penetrating renewable energy systems. However, owing to the intermittent and variable nature of the wind, the power output from WTGs is subject to fluctuations. This variability can impact the grid stability, particularly in terms of frequency regulation. Therefore, ensuring that WTGs operate within acceptable frequency limits is crucial for maintaining a reliable and stable power supply.

### F. SOLAR PHOTOVOLTAIC

Solar PV systems convert sunlight into electricity using photovoltaic cells [43]. These cells are typically composed of semiconducting materials that generate DC when exposed to sunlight. Solar PV systems are crucial components of renewable energy generation, harnessing clean and abundant solar energy to produce electricity [44]. They play a crucial role as primary renewable energy sources within highly penetrating systems. They consist of arrays of photovoltaic (PV) panels that capture solar energy and convert it into usable electrical energy. Generated electricity can be consumed locally within the system or supplied to the primary grid. Similar to WTGs, PV systems can also exhibit randomness in the sunlight intensity. To capture this stochastic behavior accurately, PV systems can be modelled by incorporating low-pass filtered white noise signals, as shown Figure 8 [45].

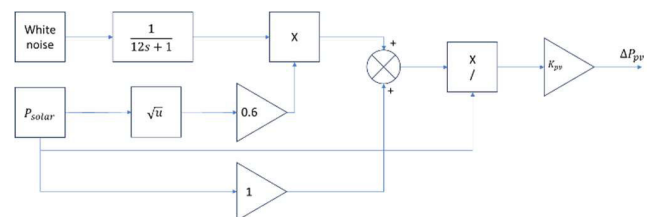


FIGURE 8. Dynamic model of solar photovoltaic.

This modelling approach allows for the consideration of variations in sunlight intensity, which directly impacts the power output of the PV system. By incorporating a low-pass filter, high-frequency fluctuations in sunlight intensity were

attenuated, mimicking the smoothing effect of real-world conditions. As a result, this modelling technique enables a more realistic representation of the PV system performance, facilitating the accurate analysis and optimization of solar power generation. Incorporating uncertainty modelling techniques in PV systems is crucial for various applications such as grid integration studies, energy yield assessment, and system design optimization. In addition, it helps in assessing the system reliability, evaluating the impact of variable weather conditions, and developing strategies to improve the overall efficiency and stability of the PV system.

By incorporating uncertainty modelling into PV system analysis, researchers and engineers can make informed decisions and devise strategies to maximize the utilization of solar energy resources, leading to a more sustainable and resilient energy future.

**G. AGGREGATED ELECTRIC VEHICLE**

An electric vehicle, commonly known as an EV, is an automobile driven by one or more electric motors that employs energy deposited in rechargeable batteries. EVs are part of the growing trend towards sustainable transportation and have gained popularity owing to their reduced carbon emissions and reliance on renewable energy sources. EVs are considered a means of transportation and a valuable asset that can actively support stability and regulation. Furthermore, EVs accommodate bidirectional power flow, allowing them to consume electricity from the grid and supply excess energy back to the grid when required [46].

The SoC-dependent battery model developed for a New Generation of Vehicles (PNGV), as shown in Figure 9, provides a comprehensive representation of the characteristics and behavior of EV batteries. It is designed to accurately simulate EV battery performance, energy storage, and power capabilities, enabling precise control coordination strategies.

For energy storage, the current discharged by the EV can be modelled as a function of the frequency deviation  $I_0 = f(\Delta f)$ , whereas its no-load voltage ( $V_0$ ), series resistance ( $R_0$ ), parallel resistance ( $R_p$ ), and parallel capacitance ( $C_p$ ) are functions of the SoC [47]. Using quadratic regression, the

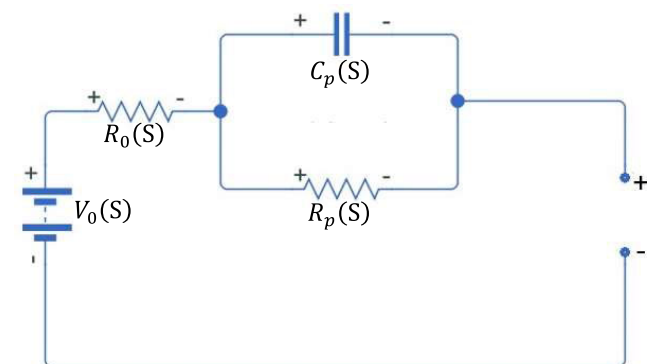


FIGURE 9. PNGV battery model.

SoC-dependent parameters are shown in (1)–(4). By utilizing quadratic regression instead of a look-up table, the complexity and computational burden were reduced significantly.

$$V_0(S) = 0.4389S^2 - 0.01304S + 3.696 \tag{1}$$

$$R_0(S) = 5.106S^2 - 8.747S + 9.688 \tag{2}$$

$$C_p(S) = -1.876S^2 + 0.2097S + 1.783 \tag{3}$$

$$R_p(S) = 5.26S^2 - 5.986S + 7.735 \tag{4}$$

where  $S$  is the SoC of EV in percentage.

The PNGV battery model captures important parameters and nonlinear relationships and accurately represents battery behavior. The model enables the accurate prediction and control of battery performance, maximizing battery efficiency and lifespan. By integrating the model into the optimization process, decisions on charging, discharging, and energy management strategies can be made. The model also facilitates the integration of EV batteries as flexible assets, enhancing power balance, frequency stability, and overall reliability. Its significance lies in enabling effective control coordination, optimizing battery utilization, contributing to stability, and extending EV battery lifespan.

The concept of an aggregated EV fleet essentially involves viewing it as a collective entity composed of individual EVs. This collective behavior can be mathematically represented by considering the multiplication of individual dynamic models, providing a comprehensive understanding of the entire EV population. In essence, when translating frequency deviations into power adjustments, this aggregated behavior is encapsulated by a specific factor denoted as  $K_{ev}$  as depicted in Figure 10.

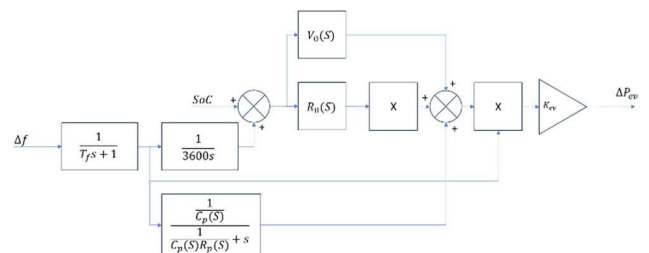


FIGURE 10. Dynamic model of the aggregated EV.

**IV. CONTROL STRATEGIES**

**A. OPTIMAL ROBUST-PID CONTROL**

PID control is a widely used control strategy that adjusts the output of a system based on the proportional, integral, and derivative components of the error between the desired and actual system states [48]. Optimizing the PID controller parameters enables control coordination to minimize the frequency deviations and maintain the desired frequency set-point. Optimal control refers to the process of determining control inputs that optimize the performance of a system according to a specified objective function [49]. Optimal PID control combines the principles of PID control and optimal

control. It aims to determine the optimal PID controller parameters that regulate the system frequency effectively and meet specific optimization criteria [50]. Adjusting the proportional, integral, and derivative gains of the PID controller allows the system to respond optimally to disturbances, minimize frequency deviations, and achieve the desired performance objectives.

The Integral of Time-weighted Squared Error (ITSE) given in (5) is a widely used performance measure in control systems for assessing the effectiveness of the PID control strategy [51]. It offers several advantages over other performance indicators such as the Integral of Time-weighted Absolute Error (ITAE), Integral of Absolute Error (IAE), and Integral of Squared Error (ISE).

$$ITSE = \int_0^{t_f} t \cdot e(t)^2 dt \quad (5)$$

where:

$e(t)$  represents the error at time  $t$ .

$t$  is time.

$t_f$  is the final time.

One of the main advantages of the ITSE performance index is its ability to provide more weight to sustained deviations from the desired frequency setpoint [52]. ITSE captures the magnitude and duration of frequency deviations by squaring the error term and integrating it over time. This is particularly valuable in applications where sustained deviations can have significant consequences, such as in power systems, where frequency stability is crucial.

The weighting of the squared error over time in the ITSE index allows it to effectively penalize long-lasting frequency deviations. This contrasts with performance indices such as ITAE and IAE, which focus primarily on the absolute magnitude of the error without considering its duration. Furthermore, by emphasizing sustained deviations, ITSE provides a more comprehensive evaluation of the control performance and highlights the need for an efficient and prompt correction of frequency deviations.

In real-world scenarios, uncertainties are associated with the system parameters and states, which can affect the performance of optimal control strategies that rely on fixed system parameters and specific inputs. Robust control techniques have been used to address these uncertainties. Robust control allows for optimization within various uncertainties, considering variations in system parameters and states [53]. This approach ensures that the resulting control strategy is optimal and resilient to changes in parameters and states within the defined range of uncertainty. By incorporating robust techniques into PID control, system performance is enhanced, providing stability and reliability even in the presence of uncertain factors.

### B. SEQUENTIAL MULTI-OBJECTIVE OPTIMISATION

Sequential Multi-objective Optimization (SMO), as formulated in (6)–(9), enhances optimization by considering

multiple control objectives sequentially. Each sub-objective can be assigned different weights  $w_n$  as a part of the primary objective function  $f_n$ . This approach involves iterative exploration of the control parameter space using an optimization algorithm to find solutions that achieve optimal trade-offs among multiple objectives [54].

$$\min_x f(x) = (f_1(x) w_1 [u(t-t_0) - u(t-t_1)], \dots, f_n(x) w_n [u(t-t_{n-1}) - u(t-t_n)]) \quad (6)$$

$$g_i(x) \leq 0, \quad i = 1, 2, \dots, p \quad (7)$$

$$h_j(x) = 0, \quad i = 1, 2, \dots, q \quad (8)$$

$$lb_i \leq x_i \ \& \ \leq ub_i, \quad i = 1, 2, \dots, n \quad (9)$$

where:

$x$  is the vector of decision variables.

$f(x)$  represents the vector of objective functions to be minimized, consisting of  $m$  individual sequential objective functions  $f_1(x), f_2(x), \dots, f_n(x)$ .  $w_n$  is the weighting coefficient for the objective function  $f_n(x)$ .  $g_i(x)$  and  $h_j(x)$  are the inequality and equality constraints, respectively.

$lb_i$  and  $ub_i$  are the lower and upper bounds for each decision variable  $x_i$ .

$p$  and  $q$  represent the number of inequality and equality constraints, respectively.

$$u(t-t_{n-1}) - (t-t_n) \text{ is a time window for } f_n(x).$$

The objective is to determine the optimal vector of decision variables  $x$  that minimizes the objective functions  $f(x)$  while satisfying the constraints.

### C. SEQUENTIAL QUADRATIC PROGRAMMING

Sequential Quadratic Programming (SQP), as in (10), is known for its fast convergence rate, making it suitable for solving optimization problems efficiently [55]. Furthermore, SQP effectively handles equality and inequality constraints, ensuring that the control coordination satisfies the system requirements and constraints. Furthermore, SQP provides locally optimal solutions by iteratively approximating the problem using quadratic models, resulting in improved control coordination [56].

$$\min_{\Delta x} \frac{1}{2} \Delta x^T P_k \Delta x + q_k^T \Delta x \quad (10)$$

where:

$\min_{\Delta x}$  represents the minimization operator with respect to  $\Delta x$ , which is the optimisation variable.

$P_k$  is the Hessian matrix at iteration  $k$ , which represents the second-order derivative of the objective function.

$q_k$  is the gradient vector at iteration  $k$ , which represents the first-order derivative of the objective function

The quadratic programming subproblem aims to find the optimal value of  $\Delta x$  that minimises the quadratic function  $\frac{1}{2} \Delta x^T P_k \Delta x + q_k^T \Delta x$ . This subproblem is solved at each iteration of the SQP algorithm to update the search direction and move towards the optimal solution of the original



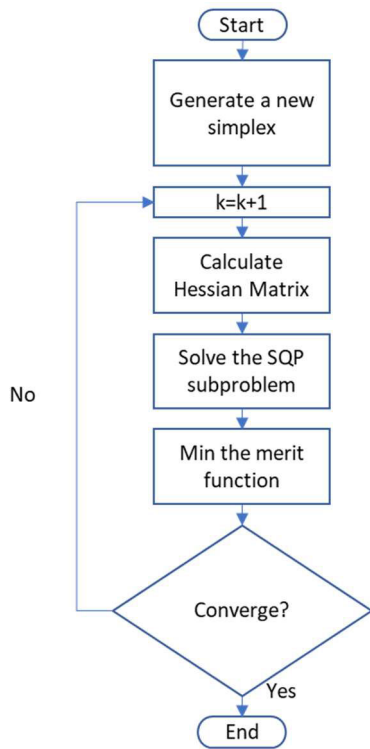


FIGURE 11. Flowchart of SQP algorithm.

optimization problem. The flowchart of the SQP algorithm is given in Figure 11.

**D. SIMPLEX ALGORITHM**

The Simplex algorithm (11) is known for its robustness in handling many optimization problems, including linear programming problems. Furthermore, the simplex performs well even for high-dimensional optimization problems, making it suitable for complex control coordination tasks. In addition, the simplex algorithm provides insights into the intermediate steps of the optimization process, allowing for a better understanding and interpretation of the results.

$$\min_x c^T x \tag{11}$$

where:

$\min_x c^T x$  represents the minimisation operator with respect to the variable vector  $x$  and  $c$  is the objective function coefficient vector.

The simplex algorithm aims to determine the optimal value of  $x$  that minimizes the objective function  $c^T x$ .

The algorithm iteratively explores feasible solutions by moving along the edges of the feasible region defined by constraints [57]. It continues to iterate until it reaches the optimal solution or until it determines that the problem is unbounded. A flowchart of the simplex algorithm is shown in Figure 12 [58].

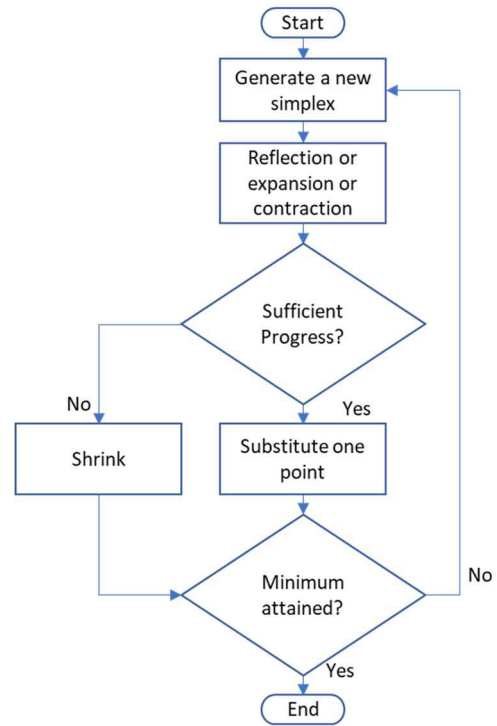


FIGURE 12. Flowchart of the simplex algorithm.

**E. INTERIOR POINT ALGORITHM**

Interior Point (IP) algorithms offer efficient solutions for large-scale optimization problems, making them suitable for complex control coordination tasks. Furthermore, IP algorithms effectively handle inequality constraints, allowing the incorporation of constraints related to renewable energy operational limits. In addition, IP algorithms often provide high-quality solutions by exploring the interior of the feasible region, leading to improved control-coordination outcomes. The IP algorithm has the same formulation as the simplex. The difference is that the IP operates within the interior of the feasible region [59]. It searches for the optimal solution by iteratively moving towards the optimal point while satisfying the constraints.

**F. PATTERN SEARCH ALGORITHM**

Pattern Search (PS) is a derivative-free optimization method that does not rely on gradient information [60], [61]. This is advantageous when dealing with optimization problems where the objective function is not differentiable or the gradients are difficult to compute. Instead of using derivatives, pattern-search optimization explores the search space by iteratively evaluating the objective function at different points based on a predefined pattern or set of rules. A flowchart of the pattern search algorithm is shown in Figure 13 [62].

**V. METHODOLOGY**

The control coordination of the EV aggregator as C-FCAS aims to guarantee the stability and reliability of the system

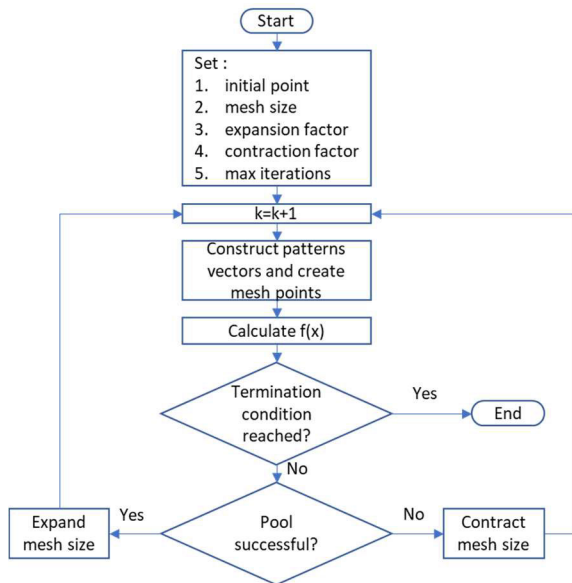


FIGURE 13. Flowchart of pattern search algorithm.

frequency by regulating the power output of EVs. In this research, a Step Load Perturbation (SLP) of 0.1 pu is introduced to the system, causing a frequency contingency event [63], [64], [65]. This perturbation disrupts the stability of the system and necessitates corrective response. The EV aggregator is employed to address this event by utilizing a sequential approach with two primary objectives.

The first objective of the control strategy is to mitigate the frequency perturbation induced by the SLP. The objective is to restore the frequency of the system to its desired operating range by adjusting the power output of the EV aggregator. This objective plays a significant role in maintaining stability and reliability during and after a contingency event. The second objective is to restore the power discharged by the EV aggregator to zero. This objective ensures that the power generated by the EV aggregator is utilized effectively. By restoring the power to zero, the control strategy enables smooth transition and prevents abrupt changes in the power output of the EV aggregator, which can adversely affect the stability of the system.

A sequential approach, consisting of two phases, was adopted to achieve these objectives. The duration of the first objective sequence was set to 6 s and 60 s, aligned with the specific market conditions in Australia. These durations were chosen based on the time required to effectively address the frequency perturbation in the respective markets and the seldomness of 5 min of C-FCAS occurrence [66]. After completing the first objective sequence, the second objective is introduced, with a consistent duration of 60 seconds for both markets. This duration assumes that, within this time window, the system and its components have reached a new steady state, where the frequency has been stabilized, and the power discharged by the EV aggregator has been restored to zero.

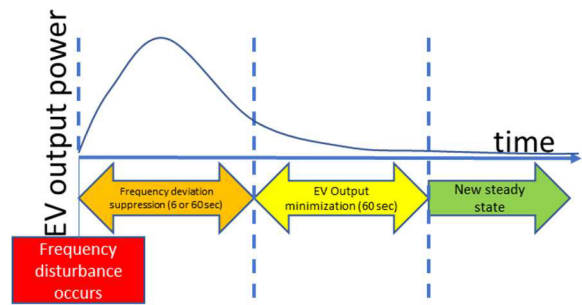


FIGURE 14. Design of simulation.

Figure 14 provides a visual representation of the sequential approach and duration of each objective. It illustrates the timeline of the event, including the occurrence of the SLP, initiation of the control strategy, and completion of each objective. This timeline serves as a reference for understanding the temporal aspects of the control strategy and its response to the frequency of contingency events.

The optimization process commences by initializing the PID controller gains and simulating the system response. Subsequently, the performance of the system was evaluated using combination of multiple ITSE; ITSE of frequency deviation during first window and ITSE of zero power output during the second. MATLAB Response Optimizer app is employed for conducting this procedure. The controller gains are then iteratively adjusted to enhance the control performance. This iterative process continues as the optimization algorithm searches for better solutions by refining the PID gains based on the ITSE performance index. The objective is to obtain a set of controller gains that yields satisfactory control performance.

Multiple optimization algorithms were applied to determine the most effective algorithm. While the ITSE index is used as the objective function for optimization, the parameters used to compare the algorithms are the frequency nadir (the lowest point the frequency reaches) and Rate of Change of Frequency (RoCoF). These parameters are commonly used by power utilities to assess the effectiveness of C-FCAS [67]. However, for computational purposes, it is more convenient to utilize the ITSE index instead of directly considering the frequency nadir and RoCoF. This approach allows for a comprehensive evaluation of the control strategies while facilitating the analysis and comparison of the optimization results.

Finally, the identified best algorithm optimizes the PID parameters, thereby ensuring the optimal performance of the control strategy. However, to enhance the robustness of the control approach, the optimization process considers several uncertainties that can affect the behavior of the system. These uncertainties include variations in the SoC of the energy storage system and magnitude of the SLP.

SoC uncertainty accounts for different levels of energy stored in the system, ranging from low to high SoC values.

This variability reflects real-world scenarios in which the energy-storage capacity of EVs or other storage systems may vary. By incorporating this uncertainty, the control strategy can adapt to different energy-storage conditions and ensure reliable performance across various operating states. The uncertainty in the magnitude of the SLP acknowledges the variability in power consumption patterns within the grid. By considering different SLP magnitudes, the control strategy can effectively respond to varying load demands, thereby ensuring stable and efficient frequency regulation. By incorporating these uncertainties into the optimization process, the control strategy is designed to be robust and adaptable, ensuring its effectiveness under various operating conditions. The inclusion of uncertainties allows for a comprehensive evaluation of the performance of the control strategy and ensures its ability to handle real-world uncertainties in a power grid.

## VI. RESULTS AND DISCUSSIONS

### A. ALGORITHMS COMPARISON

In this subsection, several optimization algorithms are tested. Among the optimization techniques provided by the MATLAB Response Optimizer app, the SQP, PS, Simplex, and IP algorithms have demonstrated successful convergence. However, other algorithms such as Trust Region Reflective (TRF), Active Set (AS), and Nelder-Mead (NM) did not achieve convergence in this implementation. The results are presented in Table 1, Table 2, Table 3 and Table 4, corresponding to the 6-sec market optimization, 6-sec market simulation, 60-sec market optimization, and 60-sec market simulation, respectively. The purpose of these tests was to evaluate the performance of the different algorithms in achieving the optimal frequency nadir and restoring the EV aggregator to its stable idle state.

TABLE 1. Optimization result for 6-sec market.

No	Algorithm	$K_p$	$K_i$	$K_d$
1	IP	-13.65	-0.23	-6.38
2	PS	-6.14	-	-58.19
3	Simplex	-2.06	-0.06	-5.72
4	SQP	-13.09	0.25	-3.90

TABLE 2. Simulation result for 6-sec market.

Algorithm	Final EVA Out (pu)	Freq Nadir (Hz)	RoCoF Min (Hz/s)	RoCoF Max (Hz/s)
IP	$1.44 \times 10^{-2}$	-5.72	-25.21	4.58
PS	$2 \times 10^{-4}$	-2.84	-25.63	0.415
Simplex	$3 \times 10^{-3}$	-9.03	-25.17	2.465
SQP	$-1.6 \times 10^{-3}$	-7.05	-25.16	7.42

Among the algorithms tested in both markets, the Pattern Search (PS) algorithm demonstrated superior performance in

TABLE 3. Optimization and simulation result for 60-sec market.

Algorithm	$K_p$	$K_i$	$K_d$
IP	-1.23	0.39	-1.08
PS	-38.28	0.11	-262.41
Simplex	-2.08	0.36	-1.21
SQP	-74.31	0.42	-3.60

TABLE 4. Simulation result for 60-sec market.

Algorithm	Final EVA Out (pu)	Freq Nadir (Hz)	RoCoF Min (Hz/s)	RoCoF Max (Hz/s)
IP	$-1 \times 10^{-4}$	-16.91	-25.08	9.23
PS	$-3.1 \times 10^{-3}$	-0.81	-25.98	13.08
Simplex	$1.2 \times 10^{-2}$	-15.38	-25.08	7.68
SQP	$-3.3 \times 10^{-3}$	-3.95	-25.28	19.58

achieving an optimal frequency nadir. It consistently outperformed the other algorithms in terms of minimizing frequency deviations during the optimization process. In addition, the PS algorithm effectively brought the EV aggregator back to its stable idle state, ensuring its proper functioning and contributing to the smooth operation of the system.

However, it is essential to note that the Sequential Quadratic Programming (SQP) algorithm failed to meet the desired results for the 6-sec market, as depicted in Figure 15 (top). This indicates that the SQP algorithm is not as effective in minimizing the frequency deviations and restoring the system stability within a given time window. Similarly, the Interior Point (IP) and simplex algorithms also fell short of meeting the requirements of the 60-second market, as shown in Figure 16 (top). These algorithms cannot effectively optimize the response of the system or stabilize the frequency within the desired timeframe.

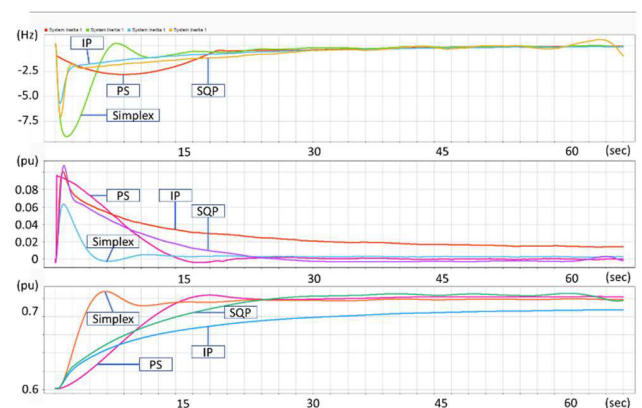


FIGURE 15. Simulation result for 6-sec market. Frequency deviation (top), EV aggregator output (middle), generator (bottom).

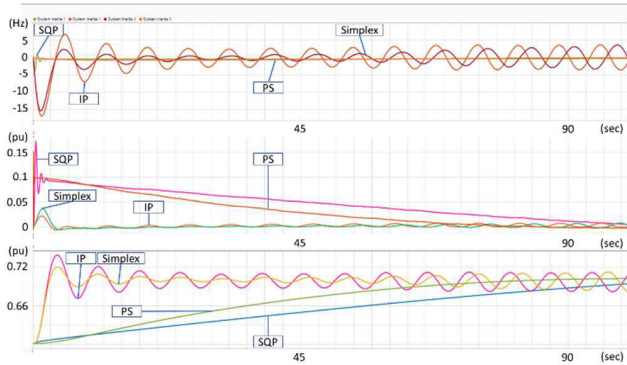


FIGURE 16. Simulation result for the 60-sec market. Frequency deviation (top), EV aggregator output (middle), generator (bottom).

The success of returning an EV aggregator to its stable idle state is an essential factor that influences the overall performance. The ability to bring the EV aggregator back to its idle state efficiently ensures a smooth loading transition for the generator, as depicted in Figure 15 (bottom) and Figure 16 (bottom).

The PS algorithm consistently achieved this outcome, highlighting its superiority in optimizing system performance and maintaining stability. These findings underscore the significance of selecting an appropriate optimization algorithm for C-FCAS control. The PS algorithm proved to be a robust and reliable choice, showing its effectiveness in achieving the desired objectives of frequency deviation minimization and restoring the EV aggregator to its stable idle state.

**B. VARIATION OF OBJECTIVE FUNCTION WEIGHTING**

Considering the superior performance of the PS algorithm, two scenarios were simulated by adjusting the weighting of the objective functions in both the 6-second and 60-second markets. In the first simulation, the first objective function was assigned a weight five times greater than that of the second objective (5:1), focusing on effective system frequency deviation suppression.

In the second simulation, the weight of the second objective function was increased by a factor of five compared to the first objective (1:5), emphasizing the suppression of the EV aggregator output. This strategic weighting allows for a comprehensive exploration of the optimization problem, addressing both frequency stability and efficient EV aggregator utilization.

As expected, under the 5:1 weighting condition, the frequency nadir reached its lowest value compared to the other conditions, indicating the successful minimization of frequency deviations. However, the suppression of the EV aggregator output is less effective under this weighting condition because of its lower priority. Conversely, under the 1:5 weighting condition, the frequency nadir was higher, indicating a less successful reduction in the frequency deviations. However, the suppression of the EV aggregator output is more

TABLE 5. Optimization and result for objective weighting variations for 6-sec market.

$w_1:w_2$	$K_p$	$K_i$	$K_d$	Final EVA Out (pu)	Freq Nadir (Hz)	RoCoF Min (Hz/s)	RoCoF Max (Hz/s)
1:1	-6.1	-	-58.2	$2 \times 10^{-4}$	-2.84	-25.63	0.42
1:5	-3.8	0.02	-22.4	$-4 \times 10^{-4}$	-4.39	-25.4	0.85
5:1	-14	-	-204	$4 \times 10^{-4}$	-1.5	-26.07	7.87

TABLE 6. Optimization and result for objective weighting variations for 60-sec market.

$w_1:w_2$	$K_p$	$K_i$	$K_d$	Final EVA Out (pu)	Freq Nadir (Hz)	RoCoF Min (Hz/s)	RoCoF Max (Hz/s)
1:1	-38.3	0.11	-262.4	$-3.1 \times 10^{-3}$	-0.81	-25.98	13.08
1:5	-24.8	0.01	-264.5	$-1 \times 10^{-3}$	-1.06	-25.92	14.79
5:1	-83.6	0.64	-260.0	$1.13 \times 10^{-2}$	-0.63	-38.47	23.03

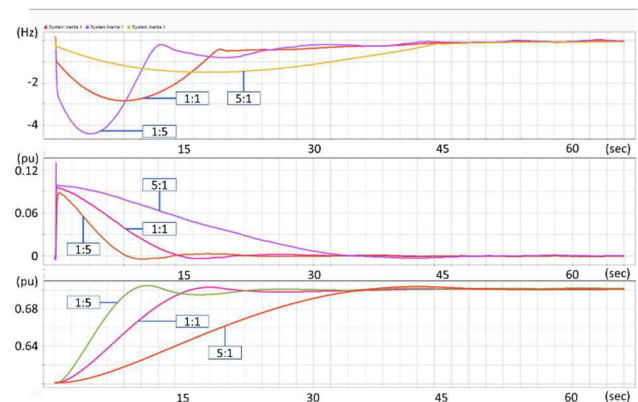


FIGURE 17. Objective weighting variations simulation results for the 6-sec market. Frequency deviation (top), EV aggregator output (middle), generator (bottom).

effective, as it is prioritized. These findings are summarized in Table 5 and Table 6.

These observations hold true for both the 6-sec and 60-sec markets, as illustrated in Figure 17 and Figure 18. The results emphasize the significance of objective function weighting in achieving the desired trade-off between minimizing frequency deviations and suppressing the EV aggregator output. The optimization process can effectively balance these objectives and yield optimal solutions by appropriately adjusting the weights.

**C. ROBUST PID CONTROL**

This subsection aims to further enhance the analysis by incorporating additional uncertainties that may influence the performance of the proposed control strategy. These uncertainties include variations in the SoC of the EV aggregatorsystem ranging from 25% to 75%. SoC represents the

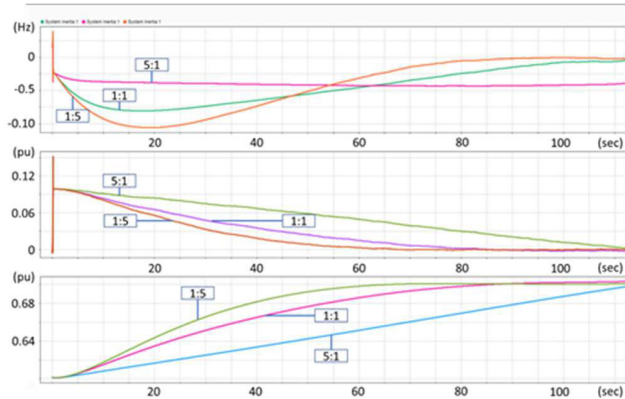


**FIGURE 18.** Different objective weighting simulation results for the 60-sec market. Frequency deviation (top), EV aggregator output (middle), generator (bottom).

**TABLE 7.** Optimization result of robust PID control for 6-sec market and 60-sec market.

Market	$K_p$	$K_i$	$K_d$
6-sec	-5.6094	0	-48.8125
60-sec	-27.6094	0	-531.4390

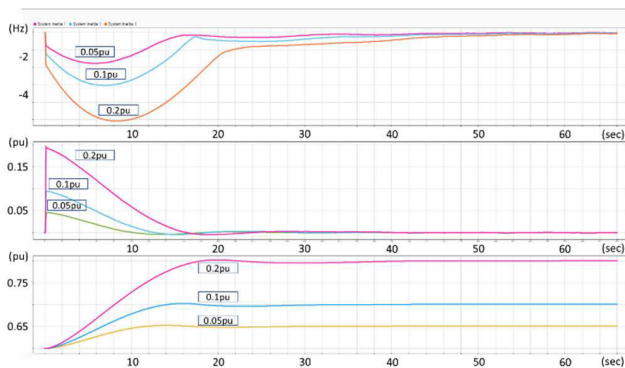


**FIGURE 19.** Robust PID control for different SLP of the 6-sec market. Frequency deviation (top), EV aggregator output (middle), generator (bottom).

energy stored in the EV aggregator and directly affects its capability to provide ancillary services.

By considering different SoC levels, this study evaluates the robustness and effectiveness of the control strategy under varying energy storage conditions. Furthermore, this research introduces uncertainties related to SLP values, which represent the expected power consumption patterns in the grid. The SLP values varied from 0.05 to 0.2 pu, representing different load demand scenarios. The study can assess the performance of the control strategy under diverse grid conditions and demand patterns by considering a range of SLP values.

Considering the range of uncertainties discussed earlier, the proposed control strategy is implemented using the SMO technique. PS optimization was chosen considering its superiority over the other tested optimization algorithms. The

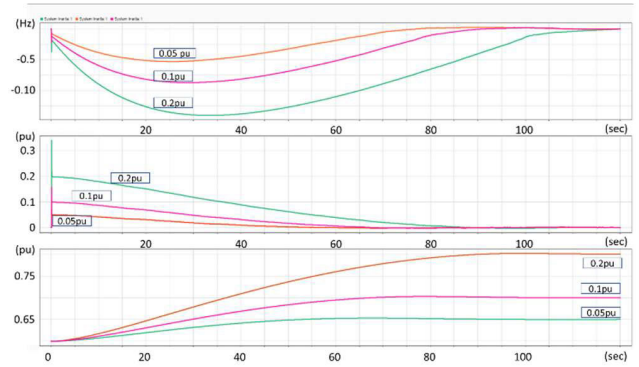


**FIGURE 20.** Robust PID control for different SLP of the 60-sec market. Frequency deviation (top), EV aggregator output (middle), generator (bottom).

control parameters obtained through SMO for the 6-sec and 60-sec markets are presented in Table 7.

The simulation results for the 6-second and 60-second market scenarios with different System Load Profile (SLP) magnitudes are presented in Figure 19 and Figure 20, respectively. These figures demonstrate the performance of the EV aggregator system as C-FCAS provider in handling varying SLP magnitudes.

## VII. CONCLUSION

In this study, the SMO technique for EV aggregator as C-FCAS was successfully implemented. Through extensive investigation, it was discovered that the combination of SMO with Pattern Search (PS) yielded superior performance compared to other combinations, namely, SMO-SQP, SMO-Simplex, and SMO-IP. The primary objective of this technique is to minimize system frequency deviation during a contingency event. However, it has been demonstrated that the SMO technique also ensures that an EV aggregator returns to its idle state after providing the required service to the grid. The EV aggregator acts as a stabilizing technology by effectively mitigating frequency deviations. This allows the generator to experience a smooth transition in loading, benefiting from the substantial time window provided by the EV aggregator. This smooth loading transition is crucial for maintaining the grid stability and reliability.

Furthermore, the SMO technique offers great flexibility by allowing adjustment of its objective function weighting. This enables the technique to be fine-tuned to accommodate specific grid and EV aggregator objectives, thereby providing a customized and optimized solution. By appropriately balancing the objectives, the SMO technique can effectively meet the operational requirements of both grid and EV aggregator systems. Moreover, a robust PID control technique can be combined with the SMO technique to address the uncertainties inherent in systems. This integration allows for the management of a wide range of uncertainties that can arise in the grid, ensuring the stability and reliability of the system under various conditions.

Regarding future research directions, the proposed technique holds promise for implementation with other similar energy storage systems, such as super-magnetic energy storage (SMES) and ultra-capacitor energy storage (UCES). Expanding the application of this approach to energy storage technologies could potentially enhance their capabilities and contributions to the power grid. Although simulation using a simplified lumped subsystem has yielded successful results, further verification using real electrical network models is essential before practical implementation in the real system. By utilizing real network models, the fulfillment of standards agreed upon by stakeholders, such as frequency nadir and RoCoF, can be further assessed. Validating the control strategy using more complex and realistic grid models will ensure its effectiveness and reliability in real-world scenarios. Moreover, considering the intricacies of actual electrical networks will allow for better insights and adjustments to optimize the performance of the strategy.

## APPENDIX

TABLE 8. Parameter value.

Subsystem	Constant	Value
EVES	$T_r$	1.2
	$K_{ev}$	0.01
	$T_{ev}$	61
PV	$K_{p1}$	-18
	$a_1$	99.5
	$b_1$	-50
	$c_1$	0.5
	$P_{solar}$	-50
	$K_{pv}$	0.2
	$C_{lpf}$	12
WTG	$P_{wf}$	1
	$K_{wind}$	0.2
Generator	$C_{lpf}$	1000
	$T_{gov}$	0.15
Load	$T_{gen}$	0.2
	$H$	0.1
	$D$	0.12
	$K_p$	0
	$K_i$	-0.03
LFC	$K_d$	0
	$\beta$	2.4

## REFERENCES

- [1] H. Yu, S. Niu, Y. Shang, Z. Shao, Y. Jia, and L. Jian, "Electric vehicles integration and vehicle-to-grid operation in active distribution grids: A comprehensive review on power architectures, grid connection standards and typical applications," *Renew. Sustain. Energy Rev.*, vol. 168, Oct. 2022, Art. no. 112812, doi: [10.1016/j.rser.2022.112812](https://doi.org/10.1016/j.rser.2022.112812).
- [2] H. S. Das, M. Nurunnabi, M. Salem, S. Li, and M. M. Rahman, "Utilization of electric vehicle grid integration system for power grid ancillary services," *Energies*, vol. 15, no. 22, p. 8623, Nov. 2022, doi: [10.3390/en15228623](https://doi.org/10.3390/en15228623).
- [3] S. de la Torre, J. A. Aguado, and E. Sauma, "Optimal scheduling of ancillary services provided by an electric vehicle aggregator," *Energy*, vol. 265, Feb. 2023, Art. no. 126147, doi: [10.1016/j.energy.2022.126147](https://doi.org/10.1016/j.energy.2022.126147).
- [4] K. Lucas-Healey, L. Jones, M. M. Haque, and B. Sturmbury. (Jan. 2021). *Electric Vehicles and the Grid*. [Online]. Available: <https://www.racefor2030.com.au>
- [5] C. Jamroen, I. Ngamroo, and S. Dechanupaprittha, "EVs charging power control participating in supplementary frequency stabilization for microgrids: Uncertainty and global sensitivity analysis," *IEEE Access*, vol. 9, pp. 111005–111019, 2021, doi: [10.1109/ACCESS.2021.3102312](https://doi.org/10.1109/ACCESS.2021.3102312).
- [6] K. Amiri, B. Mulu, M. Raisee, and M. J. Cervantes, "Load variation effects on the pressure fluctuations exerted on a Kaplan turbine runner," *IOP Conf. Ser., Earth Environ. Sci.*, vol. 22, no. 3, Mar. 2014, Art. no. 032005, doi: [10.1088/1755-1315/22/3/032005](https://doi.org/10.1088/1755-1315/22/3/032005).
- [7] D. Singh and Y. Tembhurne, "Problem of high fluctuation in speed due to reduction in extraction steam flow," *Int. J. Eng. Sci. Res. Technol.*, vol. 7, no. 3, pp. 315–322, Mar. 2018.
- [8] J. Huang and D. Yang, "Improved system frequency regulation capability of a battery energy storage system," *Frontiers Energy Res.*, vol. 10, pp. 1–10, May 2022, doi: [10.3389/fenrg.2022.904430](https://doi.org/10.3389/fenrg.2022.904430).
- [9] P. Jampheethong and S. Khomfoi, "Coordinated control of electric vehicles and renewable energy sources for frequency regulation in microgrids," *IEEE Access*, vol. 8, pp. 141967–141976, 2020, doi: [10.1109/ACCESS.2020.3010276](https://doi.org/10.1109/ACCESS.2020.3010276).
- [10] P. Li, W. Hu, X. Xu, Q. Huang, Z. Liu, and Z. Chen, "A frequency control strategy of electric vehicles in microgrid using virtual synchronous generator control," *Energy*, vol. 189, Dec. 2019, Art. no. 116389, doi: [10.1016/j.energy.2019.116389](https://doi.org/10.1016/j.energy.2019.116389).
- [11] S. Iqbal, S. Habib, N. H. Khan, M. Ali, M. Aurangzeb, and E. M. Ahmed, "Electric vehicles aggregation for frequency control of microgrid under various operation conditions using an optimal coordinated strategy," *Sustainability*, vol. 14, no. 5, p. 3108, Mar. 2022, doi: [10.3390/su14053108](https://doi.org/10.3390/su14053108).
- [12] M. Vahedipour-Dahraie, H. Rashidizaheh-Kermani, H. Najafi, A. Anvari-Moghaddam, and J. Guerrero, "Coordination of EVs participation for load frequency control in isolated microgrids," *Appl. Sci.*, vol. 7, no. 6, p. 539, May 2017, doi: [10.3390/app7060539](https://doi.org/10.3390/app7060539).
- [13] K. Kaur, N. Kumar, and M. Singh, "Coordinated power control of electric vehicles for grid frequency support: MILP-based hierarchical control design," *IEEE Trans. Smart Grid*, vol. 10, no. 3, pp. 3364–3373, May 2019, doi: [10.1109/TSG.2018.2825322](https://doi.org/10.1109/TSG.2018.2825322).
- [14] Y. Yu, O. S. Nduka, and B. C. Pal, "Smart control of an electric vehicle for ancillary service in DC microgrid," *IEEE Access*, vol. 8, pp. 197222–197235, 2020, doi: [10.1109/ACCESS.2020.3034496](https://doi.org/10.1109/ACCESS.2020.3034496).
- [15] J. Yang, Z. Zeng, Y. Tang, J. Yan, H. He, and Y. Wu, "Load frequency control in isolated micro-grids with electrical vehicles based on multivariable generalized predictive theory," *Energies*, vol. 8, no. 3, pp. 2145–2164, Mar. 2015, doi: [10.3390/en8032145](https://doi.org/10.3390/en8032145).
- [16] S. Khan, K. Mehmood, Z. Haider, M. K. Rafique, and C.-H. Kim, "A bi-level EV aggregator coordination scheme for load variance minimization with renewable energy penetration adaptability," *Energies*, vol. 11, no. 10, p. 2809, Oct. 2018, doi: [10.3390/en11102809](https://doi.org/10.3390/en11102809).
- [17] M. S. Rahman, M. J. Hossain, and J. Lu, "Coordinated control of three-phase AC and DC type EV-ESSs for efficient hybrid microgrid operations," *Energy Convers. Manage.*, vol. 122, pp. 488–503, Aug. 2016, doi: [10.1016/j.enconman.2016.05.070](https://doi.org/10.1016/j.enconman.2016.05.070).
- [18] S. Iqbal, A. Xin, M. U. Jan, M. A. Abdelbaky, H. U. Rehman, S. Salman, S. A. A. Rizvi, and M. Aurangzeb, "Aggregation of EVs for primary frequency control of an industrial microgrid by implementing grid regulation & charger controller," *IEEE Access*, vol. 8, pp. 141977–141989, 2020, doi: [10.1109/ACCESS.2020.3013762](https://doi.org/10.1109/ACCESS.2020.3013762).
- [19] J. Sabhahit, S. Solanke, V. Jadoun, H. Malik, F. García Márquez, and J. Pinar-Pérez, "Contingency analysis of a grid connected EV's for primary frequency control of an industrial microgrid using efficient control scheme," *Energies*, vol. 15, no. 9, p. 3102, Apr. 2022, doi: [10.3390/en15093102](https://doi.org/10.3390/en15093102).
- [20] R. Rana, M. Singh, and S. Mishra, "Design of modified droop controller for frequency support in microgrid using fleet of electric vehicles," *IEEE Trans. Power Syst.*, vol. 32, no. 5, pp. 3627–3636, Sep. 2017, doi: [10.1109/TPWRS.2017.2651906](https://doi.org/10.1109/TPWRS.2017.2651906).

- [21] N. Rezaei and M. Kalantar, "Smart microgrid hierarchical frequency control ancillary service provision based on virtual inertia concept: An integrated demand response and droop controlled distributed generation framework," *Energy Convers. Manage.*, vol. 92, pp. 287–301, Mar. 2015, doi: [10.1016/j.enconman.2014.12.049](https://doi.org/10.1016/j.enconman.2014.12.049).
- [22] H. R. Kermani, M. V. Dabraie, and H. R. Najafi, "Frequency control of a microgrid including renewable resources with energy management of electric vehicles," in *Proc. Iranian Conf. Renew. Energy Distrib. Gener. (ICREDG)*, Apr. 2016, pp. 114–118, doi: [10.1109/ICREDG.2016.7875905](https://doi.org/10.1109/ICREDG.2016.7875905).
- [23] H. S. Haes Alhelou, M. E. H. Golshan, and M. H. Fini, "Multi agent electric vehicle control based primary frequency support for future smart micro-grid," in *Proc. Smart Grid Conf. (SGC)*, Dec. 2015, pp. 22–27, doi: [10.1109/SGC.2015.7857385](https://doi.org/10.1109/SGC.2015.7857385).
- [24] H. Yang, H. Pan, F. Luo, J. Qiu, Y. Deng, M. Lai, and Z. Y. Dong, "Operational planning of electric vehicles for balancing wind power and load fluctuations in a microgrid," *IEEE Trans. Sustain. Energy*, vol. 8, no. 2, pp. 592–604, Apr. 2017, doi: [10.1109/TSTE.2016.2613941](https://doi.org/10.1109/TSTE.2016.2613941).
- [25] S. Maslekar, R. Venkatesh, D. Kumar, and H. Dutt Mathur, "Development of a novel strategy with electrical vehicles to mitigate frequency aberration in microgrid," in *Proc. 2nd Int. Conf. Power, Energy Environment: Towards Smart Technol. (ICEPE)*, Jun. 2018, pp. 1–5, doi: [10.1109/EPETSG.2018.8658830](https://doi.org/10.1109/EPETSG.2018.8658830).
- [26] Y. Tao, G. Wang, X. Zhang, S. Lai, Y. Wang, H. Liu, and J. Qiu, "Two-layer scheduling of aggregated electric vehicles and thermostatically controlled loads in micro-grid," in *Proc. 9th Int. Conf. Power Energy Syst. (ICPES)*, Dec. 2019, pp. 1–6, doi: [10.1109/ICPES47639.2019.9105628](https://doi.org/10.1109/ICPES47639.2019.9105628).
- [27] J. Soares, M. Silva, B. Canizes, and Z. Vale, "MicroGrid der control including EVs in a residential area," in *Proc. IEEE Eindhoven PowerTech*, Jun. 2015, pp. 141–150. [Online]. Available: <https://doi.org/10.1109/ptc.2015.7232512>
- [28] S. A. Pourmousavi and M. H. Nehrir, "Real-time central demand response for primary frequency regulation in microgrids," *IEEE Trans. Smart Grid*, vol. 3, no. 4, pp. 1988–1996, Dec. 2012, doi: [10.1109/TSG.2012.2201964](https://doi.org/10.1109/TSG.2012.2201964).
- [29] P. Lin, P. Jin, A. Zou, and Z. Wang, "Real-time identification of partnership for a new generation of vehicles battery model parameters based on the model reference adaptive system," *Int. J. Energy Res.*, vol. 45, no. 6, pp. 9351–9368, May 2021, doi: [10.1002/er.6465](https://doi.org/10.1002/er.6465).
- [30] K. Thukral, P. Wijayatunga, and S. Yoneoka, "Increasing penetration of variable renewable energy: Lessons for Asia and the Pacific," Asian Develop. Bank (ADB), Philippines, PA, USA, Tech. Rep. 1, Nov. 2017. [Online]. Available: [www.adb.org](http://www.adb.org)
- [31] C. Johnathon, A. P. Agalgaonkar, J. Kennedy, and C. Planiden, "Analyzing electricity markets with increasing penetration of large-scale renewable power generation," *Energies*, vol. 14, no. 22, p. 7618, Nov. 2021, doi: [10.3390/en14227618](https://doi.org/10.3390/en14227618).
- [32] F. Zhang, N. Liu, and J. Zhang, "Comprehensive evaluation method of microgrid planning scheme considering synergistic benefits of electric vehicles and distributed renewable energy sources," presented at the 5th Int. Conf. Electr. Distrib., 2012, pp. 1–4.
- [33] H. B. Tambunan, P. A. A. Pramana, and B. S. Munir, "Intermittent renewable energy source (IRES) model of solar energy in Cipayang microgrid system," *J. Phys. Conf. Ser.*, vol. 1402, no. 3, pp. 033103–033103, Dec. 2019. [Online]. Available: <https://doi.org/10.1088/1742-6596/1402/3/033103>
- [34] P. Nikolaidis and A. Poullikkas, "A comparative review of electrical energy storage systems for better sustainability," *J. Power Technol.*, vol. 97, no. 3, pp. 220–245, 2017. [Online]. Available: <http://papers.itc.pw.edu.pl/index.php/JPT/article/view/1096/776>
- [35] K. M. Muttaqi, Md. R. Islam, and D. Sutanto, "Future power distribution grids: Integration of renewable energy, energy storage, electric vehicles, superconductor, and magnetic bus," *IEEE Trans. Appl. Supercond.*, vol. 29, no. 2, pp. 1–5, Mar. 2019, doi: [10.1109/TASC.2019.2895528](https://doi.org/10.1109/TASC.2019.2895528).
- [36] A. Aldik and T. Khatib, "EV aggregators and energy storage units scheduling into ancillary services markets: The concept and recommended practice," *World Electr. Vehicle J.*, vol. 11, no. 1, p. 8, Dec. 2019, doi: [10.3390/WEVJ11010008](https://doi.org/10.3390/WEVJ11010008).
- [37] E. E. Michaelides, V. N. D. Nguyen, and D. N. Michaelides, "The effect of electric vehicle energy storage on the transition to renewable energy," *Green Energy Intell. Transp.*, vol. 2, no. 1, Feb. 2023, Art. no. 100042, doi: [10.1016/j.geits.2022.100042](https://doi.org/10.1016/j.geits.2022.100042).
- [38] M. G. Pollitt and K. L. Anaya, "Competition in markets for ancillary services? The implications of rising distributed generation," *Energy J.*, vol. 41, no. 1, pp. 5–32, Jun. 2020, doi: [10.5547/01956574.41.SII.MPOL](https://doi.org/10.5547/01956574.41.SII.MPOL).
- [39] AEMO. (Nov. 2021). *Guide to Ancillary Services in the National Electricity Market*. [Online]. Available: [https://aemo.com.au/-/media/files/electricity/nem/security\\_and\\_reliability/ancillary\\_services/guide-to-ancillary-services-in-the-national-electricity-market.pdf](https://aemo.com.au/-/media/files/electricity/nem/security_and_reliability/ancillary_services/guide-to-ancillary-services-in-the-national-electricity-market.pdf)
- [40] M. Bruhn, "Hybrid-geothermal-fossil electricity generation from low enthalpy geothermal resources: Geothermal feedwater preheating in conventional power plants," *Energy*, vol. 27, no. 4, pp. 329–346, 2002, doi: [10.1016/S0360-5442\(01\)00088-3](https://doi.org/10.1016/S0360-5442(01)00088-3).
- [41] P.-K. Keung, P. Li, H. Banakar, and B. Teck Ooi, "Kinetic energy of wind-turbine generators for system frequency support," *IEEE Trans. Power Syst.*, vol. 24, no. 1, pp. 279–287, Feb. 2009, doi: [10.1109/TPWRS.2008.2004827](https://doi.org/10.1109/TPWRS.2008.2004827).
- [42] M. Matsubara, G. Fujita, T. Shinji, T. Sekine, A. Akisawa, T. Kashiwagi, and R. Yokoyama, "Supply and demand control of dispersed type power sources in micro grid," in *Proc. 13th Int. Conf. Intell. Syst. Appl. Power Syst.*, 2005, pp. 67–72, doi: [10.1109/ISAP.2005.1599243](https://doi.org/10.1109/ISAP.2005.1599243).
- [43] V. Pushpabala and C. C. AsirRajan, "Case study in alternate source of load energy by photovoltaic cell in smart grid," in *Proc. Int. Conf. Smart Technol. Syst. Next Gener. Comput. (ICSTSN)*, Mar. 2022, pp. 1–5, doi: [10.1109/ICSTSN53084.2022.9761297](https://doi.org/10.1109/ICSTSN53084.2022.9761297).
- [44] R. Ciriminna, F. Meneguzzo, M. Pecoraino, and M. Pagliaro, "Solar air heating and ventilation in buildings: A key component in the forthcoming renewable energy mix," *Energy Technol.*, vol. 5, no. 8, pp. 1165–1172, Aug. 2017, doi: [10.1002/ente.201600758](https://doi.org/10.1002/ente.201600758).
- [45] J. Heidary, M. Gheisarnejad, H. Rastegar, and M. H. Khooban, "Survey on microgrids frequency regulation: Modeling and control systems," *Electr. Power Syst. Res.*, vol. 213, Dec. 2022, Art. no. 108719, doi: [10.1016/j.epsr.2022.108719](https://doi.org/10.1016/j.epsr.2022.108719).
- [46] M. A. Khan, I. Husain, and Y. Sozer, "Integrated electric motor drive and power electronics for bidirectional power flow between the electric vehicle and DC or AC grid," *IEEE Trans. Power Electron.*, vol. 28, no. 12, pp. 5774–5783, Dec. 2013, doi: [10.1109/TPEL.2013.2258471](https://doi.org/10.1109/TPEL.2013.2258471).
- [47] A. Khalil, Z. Rajab, A. Alfergani, and O. Mohamed, "The impact of the time delay on the load frequency control system in microgrid with plug-in-electric vehicles," *Sustain. Cities Soc.*, vol. 35, pp. 365–377, Nov. 2017, doi: [10.1016/j.scs.2017.08.012](https://doi.org/10.1016/j.scs.2017.08.012).
- [48] I. Carlucho, M. De Paula, S. A. Villar, and G. G. Acosta, "Incremental q-learning strategy for adaptive PID control of mobile robots," *Expert Syst. Appl.*, vol. 80, pp. 183–199, Sep. 2017, doi: [10.1016/j.eswa.2017.03.002](https://doi.org/10.1016/j.eswa.2017.03.002).
- [49] B. Foss and T. A. N. Heirung, *Merging Optimization and Control*. Philadelphia, PA, USA: Elsevier, 2016.
- [50] S. Ye and L. Sun, "Design of PID intelligent controller combining immune genetic algorithm," *J. Phys., Conf. Ser.*, vol. 1574, no. 1, Jun. 2020, Art. no. 012010, doi: [10.1088/1742-6596/1574/1/012010](https://doi.org/10.1088/1742-6596/1574/1/012010).
- [51] B. Verma and P. K. Padhy, "Optimal PID controller design with adjustable maximum sensitivity," *IET Control Theory Appl.*, vol. 12, no. 8, pp. 1156–1165, May 2018, doi: [10.1049/iet-cta.2017.1078](https://doi.org/10.1049/iet-cta.2017.1078).
- [52] H. Maghfiroh, J. S. Saputro, C. Hermanu, M. H. Ibrahim, and A. Sujono, "Performance evaluation of different objective function in PID tuned by PSO in DC-motor speed control," *IOP Conf. Ser., Mater. Sci. Eng.*, vol. 1096, no. 1, Mar. 2021, Art. no. 012061, doi: [10.1088/1757-899x/1096/1/012061](https://doi.org/10.1088/1757-899x/1096/1/012061).
- [53] X. Zhang, M. Kamgarpour, A. Georghiou, P. Goulart, and J. Lygeros, "Robust optimal control with adjustable uncertainty sets," *Automatica*, vol. 75, pp. 249–259, Jan. 2017, doi: [10.1016/j.automatica.2016.09.016](https://doi.org/10.1016/j.automatica.2016.09.016).
- [54] D. M. Roijers, P. Vamplew, S. Whiteson, R. Dazeley, D. M. Roijers, and P. Vamplew, "A survey of multi-objective sequential decision-making: a survey of multi-objective sequential decision-making," *J. Artif. Intell. Res.*, vol. 48, pp. 67–113, Jan. 2013.
- [55] A. F. Izmailov, M. V. Solodov, and E. I. Uskov, "Combining stabilized SQP with the augmented Lagrangian algorithm," *Comput. Optim. Appl.*, vol. 62, no. 2, pp. 405–429, Nov. 2015, doi: [10.1007/s10589-015-9744-6](https://doi.org/10.1007/s10589-015-9744-6).
- [56] K. Schäfer, J. Fliege, K. Flaßkamp, and C. Büskens, "Reformulating bilevel problems by SQP embedding," *PAMM*, vol. 20, no. 1, pp. 2020–2022, 2021, doi: [10.1002/pamm.202000302](https://doi.org/10.1002/pamm.202000302).
- [57] G. Sierksma and Y. Zwols, *Linear and Integer Optimization: Theory and Practice*. Boca Raton, FL, USA: CRC Press, 2015.
- [58] R. Barati, "Parameter estimation of nonlinear muskingum models using Nelder–Mead simplex algorithm," *J. Hydrologic Eng.*, vol. 16, no. 11, pp. 946–954, Nov. 2011, doi: [10.1061/\(asce\)he.1943-5584.0000379](https://doi.org/10.1061/(asce)he.1943-5584.0000379).
- [59] J.-B. Jian, H.-Q. Pan, C.-M. Tang, and J.-L. Li, "A strongly sub-feasible primal-dual quasi interior-point algorithm for nonlinear inequality constrained optimization," *Appl. Math. Comput.*, vol. 266, pp. 560–578, Sep. 2015, doi: [10.1016/j.amc.2015.05.091](https://doi.org/10.1016/j.amc.2015.05.091).

- [60] F. Güneş and F. Tokan, "Pattern search optimization with applications on synthesis of linear antenna arrays," *Expert Syst. Appl.*, vol. 37, no. 6, pp. 4698–4705, Jun. 2010, doi: [10.1016/j.eswa.2009.11.012](https://doi.org/10.1016/j.eswa.2009.11.012).
- [61] G. Naresh Kumar, M. Ikram, A. K. Sarkar, and S. E. Talole, "Hypersonic flight vehicle trajectory optimization using pattern search algorithm," *Optim. Eng.*, vol. 19, no. 1, pp. 125–161, Mar. 2018, doi: [10.1007/s11081-017-9367-0](https://doi.org/10.1007/s11081-017-9367-0).
- [62] I. Zewail, W. Saad, M. Shokair, and S. A. El-Dolil, "Maximization of total throughput using pattern search algorithm in underlay cognitive radio network," *Menoufia J. Electron. Eng. Res.*, vol. 26, no. 2, pp. 307–319, Jul. 2017, doi: [10.21608/mjeer.2017.63501](https://doi.org/10.21608/mjeer.2017.63501).
- [63] C. Mu, Y. Tang, and H. He, "Improved sliding mode design for load frequency control of power system integrated an adaptive learning strategy," *IEEE Trans. Ind. Electron.*, vol. 64, no. 8, pp. 6742–6751, Aug. 2017, doi: [10.1109/TIE.2017.2694396](https://doi.org/10.1109/TIE.2017.2694396).
- [64] Y. Zheng, Z. Huang, J. Tao, H. Sun, Q. Sun, M. Dehmer, M. Sun, and Z. Chen, "Power system load frequency active disturbance rejection control via reinforcement learning-based memetic particle swarm optimization," *IEEE Access*, vol. 9, pp. 116194–116206, 2021, doi: [10.1109/ACCESS.2021.3099904](https://doi.org/10.1109/ACCESS.2021.3099904).
- [65] A. E. Khalil, T. A. Boghdady, M. H. Alham, and D. K. Ibrahim, "Enhancing the conventional controllers for load frequency control of isolated microgrids using proposed multi-objective formulation via artificial rabbits optimization algorithm," *IEEE Access*, vol. 11, pp. 3472–3493, 2023, doi: [10.1109/ACCESS.2023.3234043](https://doi.org/10.1109/ACCESS.2023.3234043).
- [66] S. R. Thorncraft and H. R. Outhred, "Experience with market-based ancillary services in the Australian national electricity market," in *Proc. IEEE Power Eng. Soc. Gen. Meeting*, Jun. 2007, pp. 1–9, doi: [10.1109/PES.2007.385855](https://doi.org/10.1109/PES.2007.385855).
- [67] M. Saeedian, B. Pourmazarian, S. S. Seyedalipour, B. Eskandari, and E. Pouresmaei, "Emulating rotational inertia of synchronous machines by a new control technique in grid-interactive converters," *Sustainability*, vol. 12, no. 13, p. 5346, Jul. 2020, doi: [10.3390/su12135346](https://doi.org/10.3390/su12135346).



**ADLAN BAGUS PRADANA** (Student Member, IEEE) received the B.E. degree from Universitas Gadjah Mada (UGM), in 2006, and the M.Tech. degree from the Indian Institute of Technology Delhi (IIT-D), in 2012. He is currently pursuing the Ph.D. degree with The University of Queensland (UQ), Australia, with a focus on electric vehicle-grid integration and power system optimization. After gaining experience in the mining industry, he returned to his alma mater as a Lecturer.



**MD. MEJBAUL HAQUE** (Senior Member, IEEE) received the B.Sc. degree in electrical and electronic engineering (EEE) from the Rajshahi University of Engineering and Technology (RUET), in 2010, the M.Sc. degree in electrical and electronic engineering (EEE) from the Khulna University of Engineering and Technology (KUET), Bangladesh, in 2013, and the M.Eng. and Ph.D. degrees in electrical engineering from Central Queensland University, Australia, in 2016 and

2020, respectively. He is currently a Research Fellow with the School of Information Technology and Electrical Engineering, The University of Queensland (UQ), Australia. Previously, he was a Research Fellow with the School of Engineering, Australian National University, Canberra, ACT, Australia. He has authored or coauthored more than 33 technical articles, including book chapters, journals, and conference papers in electrical engineering. His research interests include power quality, power electronics, renewable energy technologies, and smart grids. He was a member of the IEEE PELS Student Subcommittee, in 2020. He was a recipient of the Thesis Academic Excellence Award for the M.Eng and Ph.D. thesis, in 2016 and 2020, respectively, and the Best Paper Award from the IEEE R10 HTC 2017. He received travel grants at the IEEE R10 HTC 2017, IEEE IAS 2019, and IEEE PESGRE 2020 conferences. He was on the Organizing Committee of past IEEE SPEC 2020 and IEEE i-COSTE 2020 as the Chair (Students Activities). He is also the Industry and Local Arrangement Co-Chair of IEEE i-COSTE 2021. He is serving as an Associate Editor for IEEE ACCESS journal. He is a registered Professional Engineer in the State of Queensland.



**AWAN UJI KRISMANTO** (Member, IEEE) was born in Malang, Indonesia. He received the B.Sc. degree in electrical engineering from Universitas Brawijaya, Indonesia, in 2004, the M.Sc. degree in electrical engineering from the Sepuluh Nopember Institute of Technology (ITS), Indonesia, in 2010, and the Ph.D. degree from The University of Queensland. Since 2005, he has been a Faculty Member with the Department of Electrical Engineering, Institut Teknologi Nasional Malang, Indonesia, Indonesia. His research interests include power electronics, distributed generation, microgrids, renewable energy integration, and stability in power systems.



**HERLAMBAng SETIADI** (Member, IEEE) received the bachelor's degree in power system engineering from Institut Teknologi Sepuluh Nopember, Surabaya, Indonesia, in 2014, the master's degree in electrical power and control engineering from Liverpool John Moores University, Liverpool, U.K., in 2015, and the Ph.D. degree from The University of Queensland. He is currently a Lecturer with the Faculty of Advanced Technology and Multidiscipline, Universitas Airlangga. His research interests include power system dynamics and control, renewable energy integration, and metaheuristic algorithms.



**MITHULAN NADARAJAH** (Senior Member, IEEE) received the Ph.D. degree in electrical and computer engineering from the University of Waterloo, Canada, in 2002. He was an Electrical Engineer with the Generation Planning Branch of Ceylon Electricity Board, Sri Lanka, and the Research Leader of Chulalongkorn University, Bangkok, Thailand. He was also a Coordinator of the Energy Field of Study and the Director of the Regional Energy Resource Information Center (RERIC), Asian Institute of Technology, Bangkok. He is currently an Associate Professor with The University of Queensland (UQ). He is also the Director of Research Training and the Postgraduate Coordinator with the School of Information Technology and Electrical Engineering, UQ. His research interests include grid integration of renewable energy and energy storage systems.